JOURNAL OF VIROLOGY, Dec. 2010, p. 12351–12361 Vol. 84, No. 23
0022-538X/10/$12.00 doi:10.1128/JVI.01598-10

Autographa californica Multiple Nucleopolyhedrovirus Ac92 (ORF92, P33) Is Required for Budded Virus Production and Multiply Enveloped Occlusion-Derived Virus Formation[▽]

Wenbi Wu and A. Lorena Passarelli*

Molecular, Cellular, and Developmental Biology Program, Division of Biology, 116 Ackert Hall, Kansas State University, Manhattan, Kansas 66506-4901

Received 30 July 2010/Accepted 14 September 2010

The *Autographa californica* multiple nucleopolyhedrovirus *orf92* (*p33*), *ac92*, is one of 31 genes carried in all sequenced baculovirus genomes, thus suggesting an essential function. Ac92 has homology to the family of flavin adenine dinucleotide-linked sulfhydryl oxidases and is related to the ERV/ALR family of sulfhydryl oxidases. The role of *ac92* during virus replication is unknown. Ac92 was associated with the envelope of both budded and occlusion-derived virus (ODV). To investigate the role of Ac92 during virus replication, an *ac92*-knockout bacmid was generated through homologous recombination in *Escherichia coli*. Titration and plaque assays showed no virus spread in *ac92*-knockout bacmid DNA-transfected insect cells. Deletion of *ac92* did not affect viral DNA replication. However, *ac92*-knockout bacmid DNA-transfected cells lacked multiply enveloped occlusion-derived nucleocapsids; instead, singly enveloped nucleocapsids were detected. To gain insight into the requirement for sulfhydryl oxidation during virus replication, a virus was constructed in which the Ac92 $C^{155}XXC^{158}$ amino acids, important for sulfhydryl oxidase activity, were mutated to $A^{155}XXA^{158}$. The mutant virus exhibited a phenotype similar to that of the knockout virus, suggesting that the C-X-X-C motif was essential for sulfhydryl oxidase activity and responsible for the altered ODV phenotype.

Baculoviruses infect insects and are characterized by a circular double-stranded DNA genome ranging from 80 to 180 kbp (10), which is packaged within a rod-shaped capsid and surrounded by an envelope. Two types of virions are produced during the baculovirus replication cycle: the budded virus (BV) and the occlusion-derived virus (ODV). Although the nucleocapsids are similar in the two, the envelopes differ in composition, reflecting their different functions during infection (4). The virions have distinct tissue tropism: ODVs infect midgut epithelial cells up to 10,000-fold more efficiently than do BVs, whereas BVs infect cultured cells 1,000-fold more efficiently than do ODVs (24).

Alphabaculovirus and *Betabaculovirus* are two genera of *Baculoviridae*, based primarily on occlusion body morphology and phylogeny (11). Alphabaculoviruses have been divided into single nucleopolyhedrovirus (SNPV) and multiple nucleopolyhedrovirus (MNPV) occlusions. The M or S refers to whether the ODVs contain multiply or singly enveloped nucleocapsids, respectively (33). The MNPVs have been isolated only from Lepidoptera (23). It has been proposed that the M phenotype has an advantage over the S phenotype. Although the establishment of primary infections may be the same, the presence of multiple virions in MNPVs accelerated the onset of systemic infections (32, 33).

The *Autographa californica* MNPV (AcMNPV) open reading frame 92 (*orf92*) (*ac92*, *p33*) is one of 31 core genes present in all sequenced baculovirus genomes (24). Previous studies showed that Ac92 and its homologs, *Culex nigripalpus* NPV *orf14* and *Helicoverpa armigera* SNPV *orf80*, are associated with the ODV (3, 8, 18). Predicted protein sequence and functional analyses indicate that Ac92 is a flavin adenine dinucleotide (FAD)-linked sulfhydryl oxidase with a conserved C-X-X-C sulfhydryl oxidase motif (15).

Coexpression of Ac92 and human P53 in insect cells leads to the interaction of the two proteins. Ac92 also enhanced P53-mediated apoptosis approximately 2-fold (20). Information on the role of Ac92 during virus replication and the significance of its interaction with P53 is lacking; thus, studying *ac92* during baculovirus replication promises to lead to insightful information.

In this study, we generated an *ac92*-knockout virus, Ac92KO-PG, to investigate the role of Ac92 during AcMNPV replication. Ac92KO-PG was compared to viruses carrying *ac92* with respect to virus production kinetics, plaque formation phenotype and production, and viral DNA and protein synthesis. Since we found that Ac92 localized to both BV and ODV, the morphology of ODVs in Ac92KO-PG was also examined by electron microscopy. In addition, to characterize *ac92*, we examined its temporal expression, identified the transcriptional initiation site, and determined protein synthesis during virus replication. In order to determine if sulfhydryl oxidase activity is responsible for the phenotypes of the knockout virus, we constructed an Ac92 mutant virus with disrupted cysteines within the motif important for sulfhydryl oxidase activity. Characterization of this virus is important to determine if this enzymatic activity is responsible for the observed phenotype and if this activity is essential for virus replication.

* Corresponding author. Mailing address: Molecular, Cellular, and Developmental Biology Program, Division of Biology, 116 Ackert Hall, Kansas State University, Manhattan, KS 66506-4901. Phone: (785) 532-3195. Fax: (785) 532-6653. E-mail: lpassar@ksu.edu.

▽ Published ahead of print on 22 September 2010.

MATERIALS AND METHODS

Viruses, cell lines, and bacterial strains. Bacmid bMON14272 (Invitrogen), herein referred to as AcBAC, containing an AcMNPV genome, was propagated in *Escherichia coli* BJ5183 as previously described (2). DH10B cells with helper plasmid pMON7124 were purchased from Invitrogen. The Sf9 insect cell line, the clonal isolate 9 from IPLB-Sf21-AE cells, derived from the fall armyworm *Spodoptera frugiperda* (31), was purchased from ATCC and cultured at 27°C in TC-100 medium (Invitrogen) supplemented with 10% fetal bovine serum, penicillin G (60 μg/ml), streptomycin sulfate (200 μg/ml), and amphotericin B (0.5 μg/ml).

RNA preparation and reverse transcription-PCR (RT-PCR). Sf9 cells were infected with AcMNPV at a multiplicity of infection (MOI) of 5. Cells were treated with the protein synthesis inhibitor cycloheximide (100 μg/ml) or DNA synthesis inhibitor aphidicolin (5 μg/ml) as previously described (9). Total cellular RNA was isolated using TRIzol reagent (Sigma) according to the protocol of the manufacturer. RNA was quantified by optical density measurements at 260 nm.

RT-PCR was performed using the Access RT-PCR System (Promega) according to the handbook provided. Two primers, Ac9251 (5′-GAGCTCATGATAC CGCTGACGCCGCT-3′) and Ac9233 (5′-TTGTATTCTCCCCATGTCATGC GT-3′), were used for PCR amplification to detect transcription of *ac92*.

5′ RACE. 5′ rapid amplification of cDNA 5′ ends (RACE) was performed using a 5′ RACE system kit, version 2.0, according to the handbook provided (Invitrogen). *ac92*-specific reverse primer Ac92SP1 (5′-CCATATCGTCGATG ATGAG-3′) and Ac92SP2 (5′-CCCATATGGTAGTAAACG-3′) were used for PCR amplification. PCR products were gel purified with a gel extraction kit (Qiagen) and cloned into pCRII (Invitrogen) prior to derivation of the nucleotide sequence.

Time course analysis of Ac92 synthesis. A monolayer of Sf9 cells (1.0×10^6) was infected at an MOI of 5 with Ac92HARep-PG, an *ac92*-knockout bacmid expressing *ac92* at a different locus (see below). The protein synthesis inhibitor cycloheximide and the DNA synthesis inhibitor aphidicolin were added as described above. At different time points, cells were collected and centrifuged at $1{,}000 \times g$ for 5 min at room temperature. The pelleted cells were washed twice with phosphate-buffered saline (PBS), pH 6.2 (19), and resuspended in PBS with an equal volume of 2× protein loading buffer (PLB; 0.25 M Tris-Cl, pH 6.8, 4% SDS, 20% glycerol, 10% 2-mercaptoethanol, and 0.02% bromophenol blue). Proteins were analyzed by SDS-12% PAGE (sodium dodecyl sulfate-polyacrylamide gel electrophoresis) followed by immunoblotting or stored at −20°C until further use.

Immunoblotting. Protein samples were mixed with equal volumes of 2× PLB and incubated at 100°C for 5 min. Samples were resolved by SDS-12% PAGE, transferred onto a polyvinylidene fluoride (PVDF) membrane (Millipore), and probed with one of the following primary antibodies: (i) mouse monoclonal antihemagglutinin (anti-HA) antibody (Covance), (ii) rabbit polyclonal VP39 antiserum (13), (iii) mouse monoclonal anti-GP64 antibody (eBioscience), or (iv) mouse monoclonal anti-IE-1 antibody; this probing was followed by incubation with the horseradish peroxidase-conjugated secondary antibodies (Sigma). Blots were developed using the SuperSignal West Pico chemiluminescent substrate (Pierce) and exposed to X-ray films.

Generation of the *ac92*-knockout bacmid. The *ac92*-knockout bacmid was generated through homologous recombination in *E. coli* as previously described (38) in which *ac92* in AcBAC was replaced with the chloramphenicol resistance gene (*Cm*). A 1,178-bp PCR fragment was amplified using pCMR (34) as the template and primers Ac92D1 (5′-AGCCTCTAAATCGACGCACCTCACCA AACTGTTGTCTTCGCAAGCAACTTACTTATACCATTTTGCGTGTCCCT TTCGTCTTCGAATAAA-3′) and Ac92D2 (5′-TGTTGTATTATTGCAAATTT AACAATTTTTTGTATTCTCCCCATGTCATGCGTTCGTAATGAGCGGG CGGTAAACCAGCAATAGACATAA-3′). This fragment contains the 1,038-bp *Cm* cassette and 70 bp of *ac92* flanking regions at each end. Purified PCR fragments (1 μg) were electroporated into electrocompetent BJ5183 cells, and colonies resistant to chloramphenicol and kanamycin were selected for further confirmation by PCR analysis. The resulting *ac92*-knockout bacmid was named Ac92KO. To facilitate further study, the Ac92KO bacmid was isolated and electroporated into DH10B cells which contained the helper plasmid pMON7124. Colonies that grew on Luria-Bertani (LB) agar plates containing 20 μg/ml chloramphenicol, 50 μg/ml kanamycin, and 10 μg/ml tetracycline were selected, and the Ac92KO bacmid was isolated and confirmed by PCR again.

PCR confirmation of the *ac92*-knockout bacmid. Four primers were used to confirm the replacement of *ac92* by *Cm* in the *ac92* locus of AcBAC. Primers Cm5 (5′-CTTCGAATAAATACCTGTGA-3′) and Cm3 (5′-AACCAGCAATA GACATAAGC-3′) were used to detect the correct insertion of the *Cm* cassette. Primers Ac9251 and Ac9231, which bind outside the flanking sequences used for recombination, were used to confirm the deleted region and the insertion of the *Cm*. Primer pairs Ac9251/Cm3 and Cm5/Ac9231 were used to examine the recombination junctions at the flanking regions upstream and downstream of the insertion site, respectively.

Construction of the *ac92* knockout, repair, and AcBAC with the *egfp* and *polyhedrin* genes. AcBAC and Ac92KO bacmids were isolated from BJ5183 cells and electroporated into DH10B cells containing the helper plasmid pMON7124. To facilitate the examination of virus-infected cells and to determine if deletion of *ac92* had any effect on occlusion morphogenesis, *polyhedrin* and *enhanced green fluorescent protein* (*egfp*) were inserted into the *polyhedrin* locus by site-specific transposition as previously described (38). To this end, several donor plasmids were constructed as follows. Two primers, Ac9252 (5′-GAGCTCAAT GCACATATGTCTTATAC-3′ with SacI restriction site underlined) and Ac9234 (5′-TCTAGAAGGTGTAGGTAACGGTACAA-3′ with XbaI restriction site underlined) were designed to amplify a 1,281-bp fragment containing the native *ac92* promoter and *ac92* open reading frame (ORF) (Ac92POA) using AcBAC DNA as a template. This PCR product was ligated into pCRII for sequencing, and the resulting plasmid, pCRII-Ac92POA, was digested with SacI and XbaI. Next, the Ac92POA fragment was inserted into the pFB1-PH-GFP plasmid (38) to generate a donor plasmid named pFB-PG-Ac92POA. Primers OppAT5 (5′-TCTAGACCGTGGTGGCGTGCGGCAA-3′ with XbaI underlined) and OppAT3 (5′-CTGCAGCGAAAATCGGGCTAGATT-3′ with PstI underlined) were designed to amplify a 473-bp fragment encoding a polyadenylation signal derived from the *Orgyia pseudosugata* MNPV inhibitor of apoptosis gene (OpIAP-pA-Tail) using plasmid pHSGFP (7) as a template. The PCR product was ligated into the pCRII vector for nucleotide sequencing, and the resulting plasmid, pCRII-OpIAP-pA-Tail, was digested with XbaI and PstI to obtain the OpIAP-pA-Tail fragment. The OpIAP-pA-Tail fragment was inserted into pFB1-PH-GFP to generate the plasmid pFB-PG-pA. Primers Ac9252 and Ac9232 (5′-TCTAGATTAGGCGTAATCTGGGACGTCGTATGGGTATTG CAAATTTAACAATTTTTTGTATTCTCCCC-3′ with XbaI restriction site underlined) were used to amplify an 1,109-bp fragment that contained the *ac92* native promoter, ORF, and an HA tag prior to the stop codon (Ac92POHA) by using AcBAC DNA as template. The PCR product was ligated into the pCRII vector for sequencing, and the resulting plasmid, pCRII-Ac92POHA, was digested with SacI and XbaI to insert the Ac92POHA fragment into pFB-PG-pA and generate a donor plasmid, pFB-PG-Ac92POHA. Electrocompetent DH10B cells containing helper plasmid pMON7124 and AcBAC were transformed with pFB1-PH-GFP to generate the control bacmid AcWT-PG. Electrocompetent DH10B cells containing helper plasmid pMON7124 and Ac92KO were transformed with donor plasmid pFB1-PH-GFP, pFB-PG-Ac92POA, or pFB-PG-Ac92POHA to generate the Ac92 knockout virus Ac92KO-PG and two repair viruses, Ac92Rep-PG, with *ac92*, and Ac92HARep-PG, with an HA-tagged *ac92*. Bacmid DNA was isolated, and successful transposition was confirmed by PCR. The correct recombinant bacmids were electroporated into *E. coli* DH10B cells and screened for tetracycline sensitivity to ensure that the isolated bacmids were free of helper plasmids. Bacmid DNA was extracted and purified with the Qiagen large-construct kit and quantified by optical density measurement.

Viral growth curve analyses and plaque assays. Sf9 cells (1.0×10^6 cells/35-mm-diameter dish) were transfected with 1 μg of a bacmid construct using Grace's unsupplemented medium (Invitrogen) and Lipofectin (7). Cell monolayers were incubated for 5 h after transfection and then washed twice with TC-100 medium and replenished with 2 ml of fresh TC-100 medium supplemented with 10% fetal bovine serum. Plaque assays were performed as previously described (38). The supernatants of the transfected cells were collected at various time points to determine titers by 50% tissue culture infective dose ($TCID_{50}$) endpoint dilution assays (17) on Sf9 cells.

DNA replication analysis by quantitative real-time PCR (QPCR). To detect viral DNA replication in virus-transfected cells, QPCR was performed as previously described (30). The *gp64*-knockout virus, AcGP64KO, was used as a non-infectious control since the virus is unable to infect from cell to cell (16). Sf9 cells (1.0×10^6 cells/35-mm-diameter dish) were transfected in triplicate with 1 μg of bacmid DNA from Ac92KO-PG or AcGP64KO, and cells were collected at different time points. Total DNA was prepared with the Wizard genomic DNA purification kit (Promega) according to the protocol of the manufacturer. Purified DNA was quantified by optical density measurement. Prior to PCR, 1 μg of total DNA from each time point was digested with 20 units of DpnI restriction enzyme (NEB) overnight in a 25-μl total reaction volume. QPCR was performed with 1 μl of the digested DNA and the Absolute QPCR SYBR green fluorescein mix (Thermo Scientific) according to the protocol of the manufacturer by using the same primers to amplify a 100-bp region of the AcMNPV *gp41* as described previously (30). Standard DNA samples were used from purified AcMNPV BV DNA and serially diluted to 100, 10, 1, 0.1, 0.01, and 0.001 ng. Genomic equiv-

alents of DNA samples were determined by extrapolation from standard curves. One copy of AcMNPV genomic DNA was estimated to be 1.36×10^{-4} pg (5). A melting-curve analysis of each amplified sample was carried out to check the specificity of each reaction. The results were analyzed using GraphPad Prism version 5.01 (GraphPad Software, Inc.).

Time course analysis of viral early and late protein synthesis. To analyze the effect of deleting *ac92* on viral protein synthesis, Sf9 cells were transfected with A92KO-PG or AcWT-PG bacmid DNA. At different time points, cells were collected and samples were prepared for immunoblotting as described above. IE-1 antibodies and VP39 antisera were used as primary antibodies, and immunoblotting was performed as described above.

Purification of BV and ODV. Sf9 cells were infected with Ac92HARep-PG at an MOI of 0.01. At 96 h postinfection (p.i.), the pellet of infected cells and the supernatant were separated by centrifugation. BV was concentrated and purified as described previously (17). To collect polyhedra (4), 600 fourth-instar *Spodoptera exigua* larvae were infected by contamination of artificial diet with Ac92HARep-PG polyhedra, which were prepared from Ac92HARep-PG-infected Sf9 cells. ODVs were purified as previously described (37).

BV and ODV were fractionated into envelope and nucleocapsid fractions as previously described (4).

Electron microscopy. Sf9 cells (1.0×10^6 cells/35-mm-diameter dish) were transfected with 1 μg of bacmid DNA. Transfected cells were collected at different time points, fixed, dehydrated, embedded, sectioned, and stained as described previously (14). Samples were viewed with a Philips CM 100 transmission electron microscope at an accelerating voltage of 100 kV.

Construction of the Ac92 $C^{155}C^{158}$ to $A^{155}A^{158}$ point mutation virus. Cysteines 155 and 158 were altered to alanines by a previously described method (6) and primers Ac9255FT (5′-GCAGCCATGGCACGCGATCATTATATGAACGTCA-3′), Ac9256FS (5′-CGCGATCATTATATGAACGTC-3′), Ac9237RT (5′-TGCCATGGCTGCCTGTAGTATGAAAAATACGTTG-3′), and Ac9238RS (5′-CTGTAGTATGAAAAATACGTTG-3′) in PCRs using pCRII-Ac92POHA as a template. The PCR was started at 94°C for 3 min, followed by 25 cycles of 94°C for 20 s, 60°C for 20 s, and 68°C for 4 min, with a final 7-min extension step at 68°C. The PCR product was digested with DpnI (NEB) for 2 h and denatured at 99°C for 3 min. Hybridization was performed using two cycles of 65°C for 5 min and 30°C for 15 min. An aliquot of 20 μl from the reaction mixture was transformed into *E. coli* XL1-Blue cells. The mutations in the final product were confirmed by DNA sequencing. The correct plasmid pCRII-Ac92POHA-$C^{155}C^{158}$to$A^{155}A^{158}$ was digested with SacI and XbaI, and the mutated DNA fragment was inserted into pFB-PG-pA to generate the donor plasmid pFB-PG-Ac92POHA-$C^{155}C^{158}$to$A^{155}A^{158}$. DH10B cells containing helper plasmid pMON7124 and the Ac92KO bacmid were transformed with the donor plasmid pFB-PG-Ac92POHA-$C^{155}C^{158}$to$A^{155}A^{158}$ to generate the recombinant virus Ac92HAM1-PG. Bacmid DNA was isolated, and successful transposition was confirmed by PCR.

Expression and isolation of Ac92 and Ac92 mutant proteins in *E. coli*. The *ac92* gene was PCR amplified from plasmid pCRII-Ac92POHA using primers Ac9257 (5′-GCTAGCATGATACCGCTGACGCCGCTTT-3′ with NheI restriction site underlined) and HindIII-HA-3 (5′-AAGCTTTTAGGCGTAATCTGGGACGT-3′ with HindIII restriction site underlined), and the nucleotide sequence was confirmed. The resulting plasmid, pCRII-Ac92HA, was digested with NheI and HindIII, and the Ac92HA fragment was inserted into the pET28a vector (Novagen) to generate the expression plasmid pET28a-Ac92HA. The primers Ac9257 and HindIII-HA-3 were also used to amplify the *ac92* mutated gene using pCRII-Ac92POHA-$C^{155}C^{158}$to$A^{155}A^{158}$ as a template. The PCR product was ligated into the pCRII vector for sequencing to generate pCRII-Ac92HA-$C^{155}C^{158}$to$A^{155}A^{158}$. This plasmid was subsequently digested with NheI and HindIII, and the fragment was inserted into pET28a to generate the expression plasmid pET28a-Ac92HAM1.

For expression, BL21(DE3)/pLysS competent cells transformed with plasmid pET28a-Ac92HA or pET28a-Ac92HAM1 were grown at 30°C in LB broth containing 50 μg/ml kanamycin and 20 μg/ml chloramphenicol to an A_{600} of 0.6, induced by adding IPTG (isopropyl-β-D-thiogalactopyranoside) to a final concentration of 1 mM, and incubated overnight at 18°C. For protein purification, 2-liter cultures were harvested by centrifugation at 3,000 × *g* for 15 min at 4°C. The pellet was resuspended in 50 ml cold extraction buffer (300 mM NaCl, 50 mM $NaPO_4$, 20 mM imidazole, pH 7.5) containing a protease inhibitor cocktail tablet (Roche), and cells were disrupted by 15 10-s sonications at maximal intensity, with cooling of the sample between sonications. The lysate was clarified by centrifugation at 15,000 × *g* for 20 min at 4°C. The clarified lysate was mixed with 500 μl Talon metal affinity resin (Clontech) that had been equilibrated with extraction buffer, incubated for 3 h at 4°C with gentle agitation, transferred to a column, washed three times with extraction buffer, and eluted sequentially with 4 column volumes of extraction buffer containing 50 mM, 100 mM, 200 mM, or 300 mM imidazole.

Measurement of sulfhydryl oxidase activity. Sulfhydryl oxidase activity was measured using the method of Long et al. (15). Briefly, Ac92HA or Ac92HAM1 protein was used as an enzyme and dithiothreitol (DTT) was used as a substrate. After specific time periods, aliquots were mixed with Ellman's reagent [5,5′-dithio-bis(2-nitrobenzoic acid) (DTNB); Sigma] and thiol content was measured by absorbance at 421 nm and by calculating an extinction coefficient of 13.6 mM^{-1} cm^{-1}.

RESULTS

Activity of Ac92 as an FAD-linked sulfhydryl oxidase has been previously determined (15); however, the role of this activity during virus replication or morphogenesis is unknown. In order to determine the effects of this gene during viral replication, we constructed an *ac92*-null virus, Ac92KO-PG, and a virus with mutations within a conserved motif necessary for sulfhydryl oxidase activity, Ac92HAM1-PG. Both viruses were characterized and compared to three other viruses, AcWT-PG, carrying unaltered *ac92* at its native locus; Ac92Rep-PG, carrying *ac92* at the *polyhedrin* locus; and Ac92HARep-PG, carrying an epitope-tagged *ac92* at the *polyhedrin* locus. This approach allowed us to contrast the effects of Ac92 and its known enzymatic activity during virus replication and determine if *ac92* has a function independent of sulfhydryl oxidation.

RT-PCR analysis and mapping of the 5′ end of the *ac92* transcripts. We determined the timing of *ac92* transcription in an effort to determine when the gene was important during virus replication. RT-PCR was performed using total RNA extracted from AcMNPV-infected cells at different time points. *ac92* transcripts were detected from 9 h p.i. to 72 h p.i. (Fig. 1A, RT+). No signals were obtained when avian myeloblastosis virus (AMV) reverse transcriptase was not included (Fig. 1A, RT−). Addition of the protein synthesis inhibitor cycloheximide and DNA synthesis inhibitor aphidicolin to infected cells abolished transcription, indicting that *ac92* is a late gene, requiring DNA and prior protein synthesis (Fig. 1B).

The *ac92* transcriptional initiation site was determined by 5′ RACE analysis using total RNAs isolated from AcMNPV-infected cells at 24 h p.i. Five clones derived from the 5′ RACE products were sequenced, and transcripts were initiated at the first A of the typical baculovirus late promoter motif TAAG, located 184 nucleotides (nt) upstream of the *ac92* translation initiation codon ATG (Fig. 1C). Together, RT-PCR and the 5′ RACE analyses indicate that *ac92* is a late gene.

Synthesis of Ac92 during infection. Synthesis of Ac92 from Ac92HARep-PG was analyzed by immunoblotting lysates from Ac92HARep-PG-infected cells by using HA antibody. An immunoreactive band of approximately 33 kDa, the expected mass, was first detected at 24 h p.i. and persisted at 96 h p.i. (Fig. 1D). The protein synthesis inhibitor cycloheximide and the DNA synthesis inhibitor aphidicolin were individually added to infected cells; no proteins were detected in the presence of cycloheximide as expected, and Ac92 was not detected in aphidicolin-treated cells (Fig. 1E). The requirement for DNA synthesis indicates that Ac92 is produced at late times.

Construction of *ac92*-knockout bacmid and confirmation of its construction. Ac92KO was constructed by deleting most of

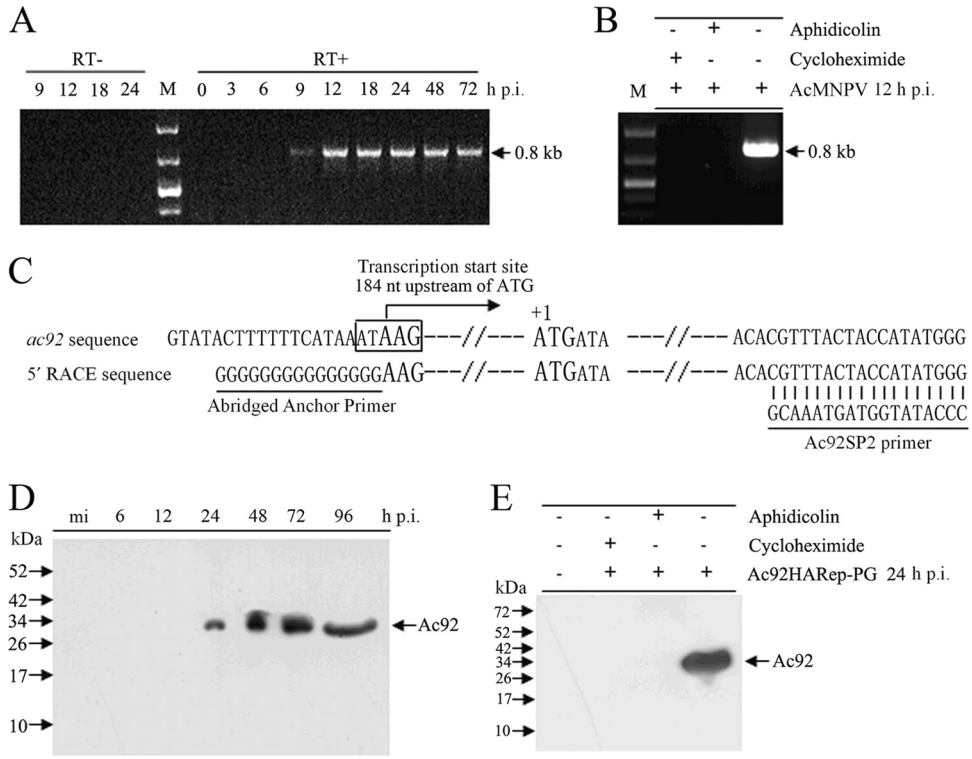

FIG. 1. Transcription kinetics of *ac92* and production of Ac92 in AcMNPV-infected cells. (A) RT-PCR analysis of *ac92* transcripts. Total RNA was extracted from AcMNPV-infected cells at designated time points. AMV reverse transcriptase was added (RT+) or omitted (RT−) as indicated. (B) Cells were infected with AcMNPV in the presence or absence of the protein synthesis inhibitor cycloheximide or the DNA synthesis inhibitor aphidicolin; RNA was extracted at 12 h p.i. and subjected to RT-PCR. (C) 5′ RACE analysis of *ac92* RNAs. The late promoter, ATAAG (boxed), and transcription initiation site (arrow) are shown. The Ac92 translation start codon is indicated as +1. Primers are underlined. (D) Cells were infected or mock infected with Ac92HARep-PG at an MOI of 5. At different times p.i. as indicated, cells were harvested, and total cellular proteins were resolved on SDS-12% PAGE gels and analyzed by immunoblotting. Transferred proteins were detected with anti-HA antibody. mi, mock-infected cells. The numbers to the left indicate the molecular masses (in kilodaltons) of protein standards. The arrow indicates the expected migration for Ac92. (E) Cells were infected with Ac92HARep-PG in the presence or absence of the protein synthesis inhibitor cycloheximide or the DNA synthesis inhibitor aphidicolin; total cellular proteins were subjected to immunoblotting with anti-HA antibody.

ac92 but retaining 150 nt from the 5′ end and 61 nt from the 3′ end of the *ac92* coding region to ensure expression of the neighboring genes, *ac93* and *ac91* (Fig. 2A). The remaining 567-nt coding sequence (nt 78762 to nt 79328 of AcMNPV [1]) was replaced with the *Cm* cassette (Fig. 2A).

PCR was performed to confirm that *ac92* had been deleted from the *ac92* locus of AcBAC and that the *Cm* cassette was inserted (Fig. 2B). Primers Ac9251 and Ac9231 were used to confirm the deletion of 567 bp within the *ac92* coding region and its replacement with the 1,038-bp *Cm*. Primer pairs Ac9251/Cm3 and Cm5/Ac9231 (Fig. 2A) were used to examine the recombination junctions upstream and downstream of *ac92*, respectively. Primers Cm5/Cm3 were used to confirm the insertion of the *Cm* cassette. The sizes of the PCR-amplified products are as expected (Fig. 2B).

Construction of Ac92KO-PG, Ac92Rep-PG, Ac92HARep-PG, and AcWT-PG AcBACs containing *polyhedrin* and *egfp*. To determine if deletion of *ac92* had any effects on occlusion morphogenesis and to facilitate examination of virus-infected cells, an *ac92*-knockout mutant, Ac92KO-PG, containing *polyhedrin* and *egfp*, was constructed by transposition of *polyhedrin* and *egfp* into the *polyhedrin* locus of Ac92KO (Fig. 2D, row i). Two repair bacmids were made to rescue and confirm the phenotype resulting from the deletion of *ac92*, Ac92Rep-PG (Fig. 2D, row ii) and Ac92HARep-PG, with an HA tag at the C terminus (Fig. 2D, row iii). AcWT-PG, AcBAC with *polyhedrin* and *egfp*, was used as a positive control (Fig. 2C). All constructs were confirmed by PCR, expression of *egfp*, and the formation of occlusions (data not shown).

Analysis of Ac92KO-PG, Ac92Rep-PG, Ac92HARep-PG, and AcWT-PG replication in bacmid DNA-transfected cells. To determine the effect of deleting *ac92* on viral replication, cells were transfected with DNA from Ac92KO-PG, Ac92Rep-PG, Ac92HARep-PG, or AcWT-PG. Transfected cells were monitored by fluorescence microscopy, and no obvious differences in the numbers of fluorescent cells and fluorescence intensities were observed at 24 h posttransfection (p.t.) (Fig. 3A, 24 h p.t.). eGFP fluorescence was observed in most AcWT-PG-, Ac92Rep-PG-, or Ac92HARep-PG-transfected cells by 72 h p.t. (Fig. 3A, 72 h p.t.). In contrast, the number of cells transfected with Ac92KO-PG DNA did not increase in eGFP fluorescence significantly from 24 to 72 h p.t. (Fig. 3A, 72 h p.t.). Inspection of cells by light microscopy showed no differences in occlusion body formation in any of the viruses up to 48 h p.t. (data not shown). However, many cells transfected with AcWT-PG, Ac92Rep-PG, or Ac92HARep-PG DNA con-

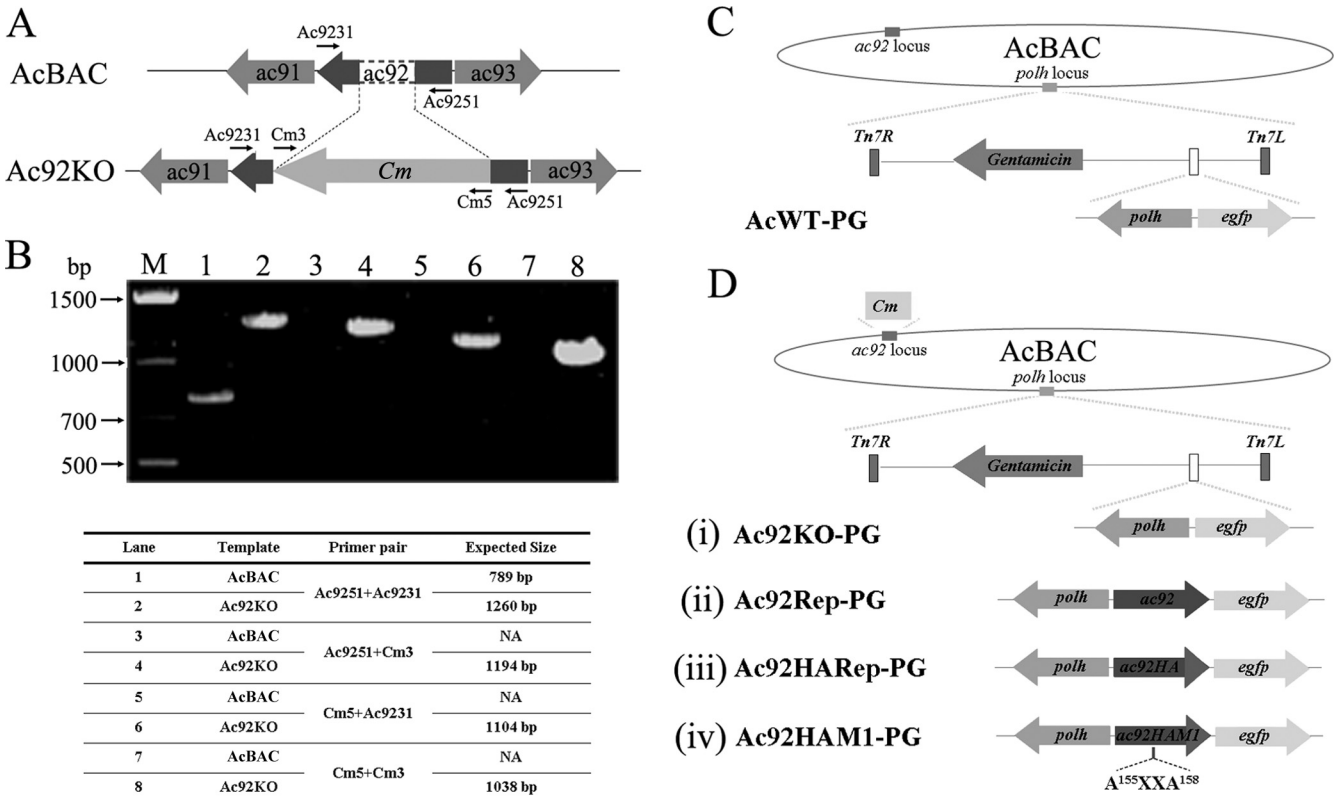

Lane	Template	Primer pair	Expected Size
1	AcBAC	Ac9251+Ac9231	789 bp
2	Ac92KO		1260 bp
3	AcBAC	Ac9251+Cm3	NA
4	Ac92KO		1194 bp
5	AcBAC	Cm5+Ac9231	NA
6	Ac92KO		1104 bp
7	AcBAC	Cm5+Cm3	NA
8	Ac92KO		1038 bp

FIG. 2. Construction of recombinant bacmids. (A) Construction strategy of Ac92KO. A fragment (567 bp) of the *ac92* ORF was deleted and replaced with the chloramphenicol resistance gene (*Cm*) between nt 78762 and nt 79328 of the AcMNPV genome (1). (B) PCR confirmation of Ac92KO. PCR primers are shown in panel A, and templates and primer sets are shown below. (C) Schematic diagram of AcWT-PG, showing *polyhedrin* (*polh*) and *enhanced green fluorescent protein* gene (*egfp*) inserted into the *polyhedrin* locus by Tn7-mediated transposition. (D) Schematic diagram of Ac92KO-PG, Ac92Rep-PG, Ac92HARep-PG, and Ac92HAM1-PG, showing *polh* and *egfp* inserted into the *polyhedrin* locus by Tn7-mediated transposition. The altered amino acids in Ac92HAM1-PG are shown below the virus, where X is any amino acid.

tained occlusion bodies by 72 h p.t., while Ac92KO-PG DNA-transfected cells showed no increase in the number of cells that contained occlusion bodies (Fig. 3A, 72 h p.t.). By 96 h p.t., most cells transfected with AcWT-PG, Ac92Rep-PG, or Ac92HARep-PG DNA showed eGFP fluorescence and contained occlusion bodies (data not shown); Ac92KO-PG DNA-transfected cells had no obvious differences, except for several small plaques (data not shown).

One-step virus growth curve analyses were performed to assess the effect of deleting *ac92* on virus replication. Cells were transfected with bacmid DNA, and at selected time points the BV titers were determined by $TCID_{50}$ endpoint dilution assays. Cells transfected with AcWT-PG, Ac92Rep-PG, or Ac92HARep-PG revealed a steady increase in virus production (Fig. 3B). However, Ac92KO-PG-infected cells had single-cell infections as indicated by single eGFP-positive cells. Accounting for single eGFP-positive cells in titers yielded a very low titer starting at 24 h p.t., where the production of BV was 10 million times less than that in *ac92*-carrying viruses at 120 h p.t. (Fig. 3B, panel ii). If single-cell infections were excluded, no detectable infectious BV was produced by Ac92KO-PG (Fig. 3B, panel i). The supernatants from Ac92KO-PG DNA-transfected cells were collected and used for subsequent infections. At 96 h p.i., only 10 to 20 individual cells per 10^6 cells were eGFP positive. Supernatant from infected cells was collected and used to infect naive cells, and by 96 h p.i., no additional eGFP-positive cells were detected (data not shown). Therefore, deletion of *ac92* is essential for budded virus production.

Plaque assays were performed to better assess virus spreading to neighboring cells. By 4 days p.t., large plaques were formed in AcWT-PG-, Ac92Rep-PG-, and Ac92HARep-PG DNA-transfected cells (Fig. 3C), while plaques from Ac92KO-PG DNA-transfected cells consisted of single cells (Fig. 3C), indicating a defect in virus production.

Quantitative analysis of viral DNA replication. To assess the role of *ac92* in viral DNA replication, we performed quantitative real-time PCR. AcGP64KO, lacking the envelope fusion protein, was used as a noninfectious control since the virus was reported to be unable to infect from cell to cell (16). Cells transfected with Ac92KO-PG or AcGP64KO bacmid DNA were harvested at 0, 24, 48, and 72 h p.t. Total intracellular DNA was extracted, and virus-specific DNA was quantified by real-time PCR (Fig. 4). We assumed that the efficiencies of viral and cellular DNA purification from viral DNA-transfected cells were equivalent. A standard calibration curve was generated, and a highly reproducible linear curve was obtained when the log concentration of purified AcMNPV genomic DNA was plotted against the cycle threshold (data not shown). Melting-curve analysis revealed that PCR products were spe-

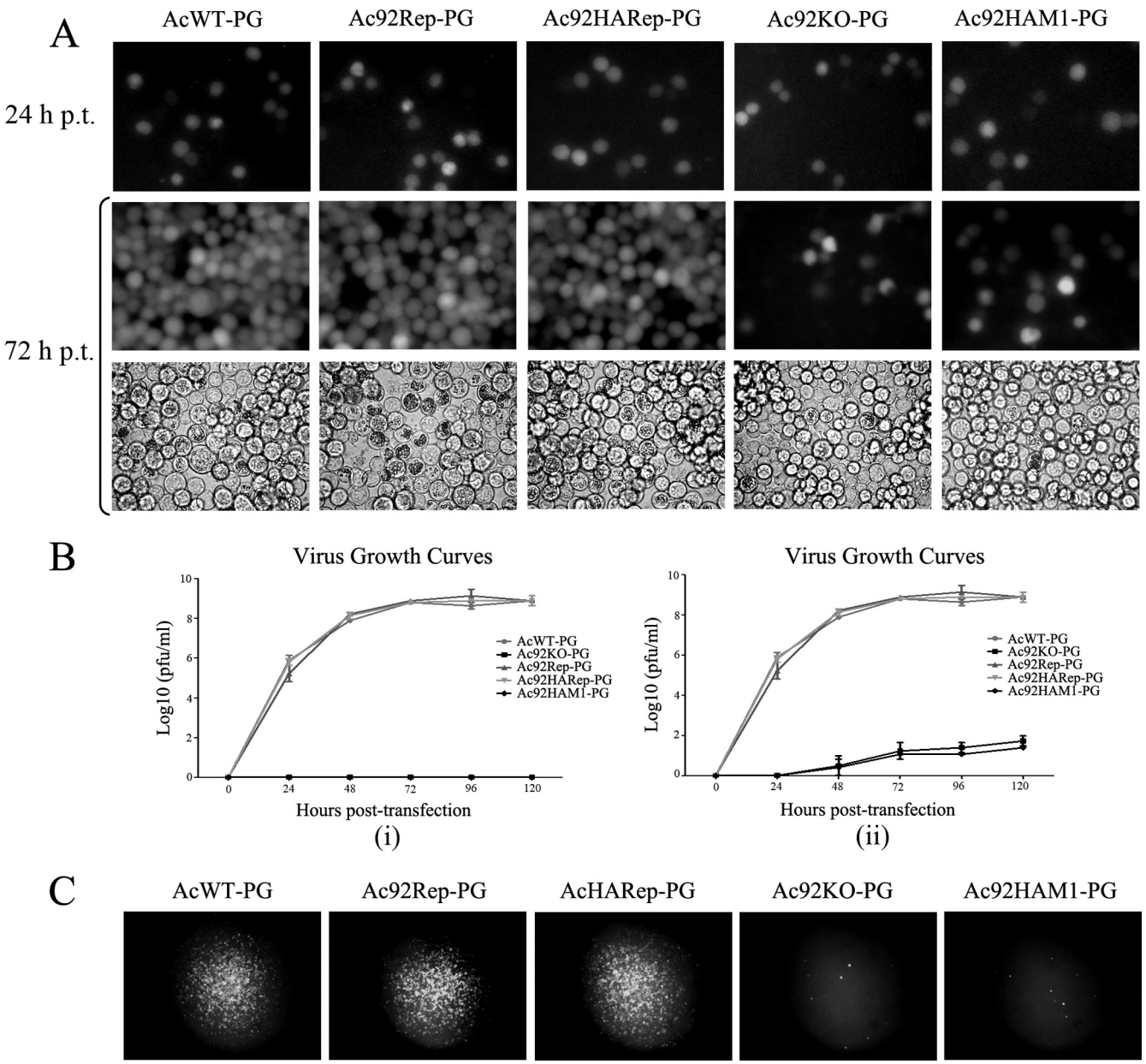

FIG. 3. Analysis of viral replication and BV production in cells. (A) The top panels show cells transfected with the indicated recombinant bacmids at 24 h p.t. The middle panels show the progression of virus infection at 72 h p.t. The bottom panels show occlusion body formation in cells in the same visual fields as those in the corresponding middle panels. (B) BV growth curves by $TCID_{50}$ endpoint dilution assays. Titers were determined from supernatants of cells transfected with AcWT-PG, Ac92KO-PG, Ac92Rep-PG, An92HARep-PG, or Ac92HAM1-PG DNA at the designated time points. Single eGFP-positive cells were not considered infected cells (i) or accounted as infected cells (ii). (C) Plaque assays using AcWT-PG, Ac92KO-PG, Ac92Rep-PG, An92HARep-PG, or Ac92HAM1-PG DNA-transfected cells.

cific (data not shown). There were no significant differences when comparing Ac92KO-PG and AcGP64KO at 0 and 24 h p.t.; however, viral DNA copy numbers were significantly higher from 0 to 24 h p.t. for each virus, clearly demonstrating that DNA replication was occurring in both viruses (Fig. 4). However, AcGP64KO produced more viral DNA at 48 h p.t. ($P < 0.001$) and 72 h p.t. ($P < 0.05$) than did Ac92KO-PG. Although it is possible that Ac92KO-PG has slight defects in DNA synthesis, we have observed that AcGP64KO has a slight leaky spreading defect that would lead to additional rounds of infections and thus more DNA copies (W. Wu and A. L. Passarelli, unpublished results) and therefore favor the later scenario.

Deletion of *ac92* does not affect IE-1 and VP39 synthesis. To evaluate the effect of deleting *ac92* on specific viral protein synthesis, proteins from AcWT-PG- or Ac92KO-PG DNA-transfected cells were harvested at designated time points and the early regulatory gene product IE-1 or the late major capsid gene product VP39 was detected with anti-IE-1 antibodies or anti-VP39 antiserum, respectively. IE-1 and VP39 were de-

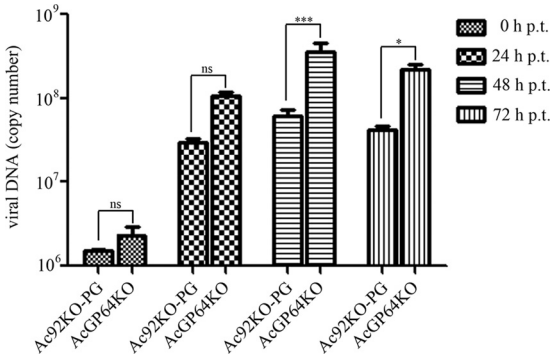

FIG. 4. Viral DNA replication. Cells were transfected with bacmid DNA in triplicate. At 0, 24, 48, and 72 h p.t., total intracellular DNA was purified, digested with DpnI, and analyzed by real-time PCR. Two-way analysis of variance was carried out with GraphPad Prism software. Bar heights indicate the averages of three repeats, and the error bars represent the standard deviations. ns, nonsignificant; ***, significant difference, $P < 0.001$; *, significant difference, $P < 0.05$.

tected from 12 h p.t. or 18 h p.t., respectively, from AcWT-PG or Ac92KO-PG DNA-transfected cells (Fig. 5). The results indicate that deletion of *ac92* did not affect IE-1 or VP39 protein production and, possibly, does not affect genes in these temporal phases.

Ac92 is localized to both BV and ODV. BV or ODV was prepared from the supernatant of Ac92HARep-PG-infected cells or whole larvae, respectively. Virions were purified and biochemically fractionated into nucleocapsid and envelope fractions (Fig. 6, lanes NC and E), and HA-tagged Ac92 was detected by immunoblotting using anti-HA antibody. Ac92 was detected in both BV and ODV and was associated with the envelope fraction of BV. In the ODV, Ac92 appeared on both nucleocapsid and envelope fractions; however, proteins in the envelope fraction are more prominent than those in the nucleocapsid fraction. At this time, we cannot rule out contamination of the ODV nucleocapsid fraction with proteins from envelopes. To confirm fractionation efficiency, the nucleocapsid protein VP39 and the BV envelope protein GP64 were also analyzed by immunoblotting, and both VP39 and GP64 were detected in the expected fractions. These results indicate that Ac92 is associated with both BV and ODV and localized to the envelope fractions.

Transmission electron microscopy analyses of Ac92KO-PG-, Ac92HARep-PG-, and AcWT-PG DNA-transfected cells. To determine whether deletion of *ac92* affected virion morphogenesis, thin sections from bacmid DNA-transfected cells were visualized by electron microscopy. At 72 h p.t., cells

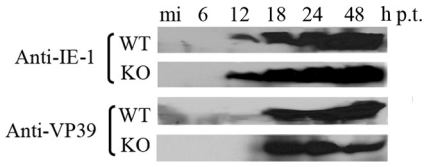

FIG. 5. Viral protein synthesis. Cells were transfected with Ac92KO-PG (KO) or AcWT-PG (WT) bacmid DNA and harvested at the designated time points. Proteins in whole-cell lysates were immunoblotted and probed with anti-IE-1 or anti-VP39.

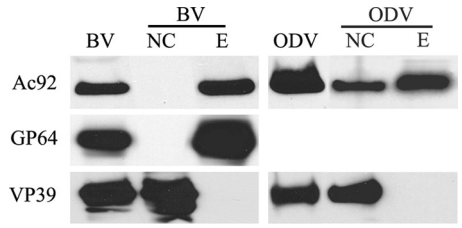

FIG. 6. Localization of Ac92 in purified and fractionated virions. BV and ODV were purified and fractionated, and proteins were detected by immunoblotting. Blots were probed with anti-HA antibody to detect Ac92, with anti-GP64 antibody to detect the BV envelope glycoprotein GP64, and with anti-VP39 antiserum to detect the major capsid protein VP39. NC, nucleocapsid fraction; E, envelope fraction.

transfected with AcWT-PG DNA showed typical characteristics of baculovirus infection, including the presence of the virogenic stroma (VS), an electron-dense net-shaped baculovirus-induced structure, containing numerous rod-shaped nucleocapsids (Fig. 7A, panel i), and virus-induced intranuclear microvesicles and bundles of enveloped nucleocapsids aligning within the ring zone (Fig. 7A, panel ii) and the mature multiply enveloped nucleocapsid within the ring zone (Fig. 7A, panel ii, arrows, and Fig. 7A, panel iii) or embedded in polyhedra (Fig. 7A, panel iv). Cells transfected with Ac92HARep-PG showed characteristics similar to those of AcWT-PG DNA-transfected cells (data not shown).

In Ac92KO-PG DNA-transfected cells, the VS and rod-shaped nucleocapsids were also observed in the nucleus (Fig. 7B, panel i). Intranuclear microvesicles appeared within the ring zone (Fig. 7B, panels ii and iv). However, ODVs with multiply enveloped nucleocapsids were not detected in the ring zone; instead, ODVs with singly enveloped nucleocapsids accumulated along with the microvesicles (Fig. 7B, panels ii and iv). The shape and the size of polyhedra formed after transfection of cells with Ac92KO-PG DNA were similar to those of polyhedra formed by AcWT-PG or Ac92HARep-PG DNA-transfected cells; however, some did not contain ODVs (Fig. 7B, panel vi), at least in the cross sections viewed, and some contained ODVs with singly enveloped nucleocapsids (Fig. 7B, panel v). Together, these observations indicate that deletion of *ac92* did not affect the formation of the VS, nucleocapsids, or polyhedra. However, it affected the formation of ODVs with multiply enveloped nucleocapsids. To our knowledge, *ac92* is the only gene affecting this step in virion assembly.

Construction and characterization of the Ac92 $C^{155}XXC^{158}$ to $A^{155}XXA^{158}$ point mutation virus Ac92HAM1-PG. *ac92* encodes an FAD-linked sulfhydryl oxidase, a member of the ERV1/ALR family of sulfhydryl oxidases (15). The presence of a C-X-X-C active-site motif, where X is a variable amino acid, is the hallmark of proteins that are involved in forming or breaking disulfide bonds (29). To assess whether the C-X-X-C motif in Ac92 is essential for sulfhydryl oxidase activity and to determine the effects of this activity on virus morphogenesis, Ac92HAM1-PG, in which the predicted cysteine amino acids 155 and 158 of Ac92 were mutated to alanines and an HA tag was inserted at the C terminus of *ac92*, was constructed. The *ac92* in Ac92HAM1-PG was driven by the *ac92* native promoter, and the virus carried *polyhedrin* and *egfp* at the *polyhedrin* locus (Fig. 2D, row iv).

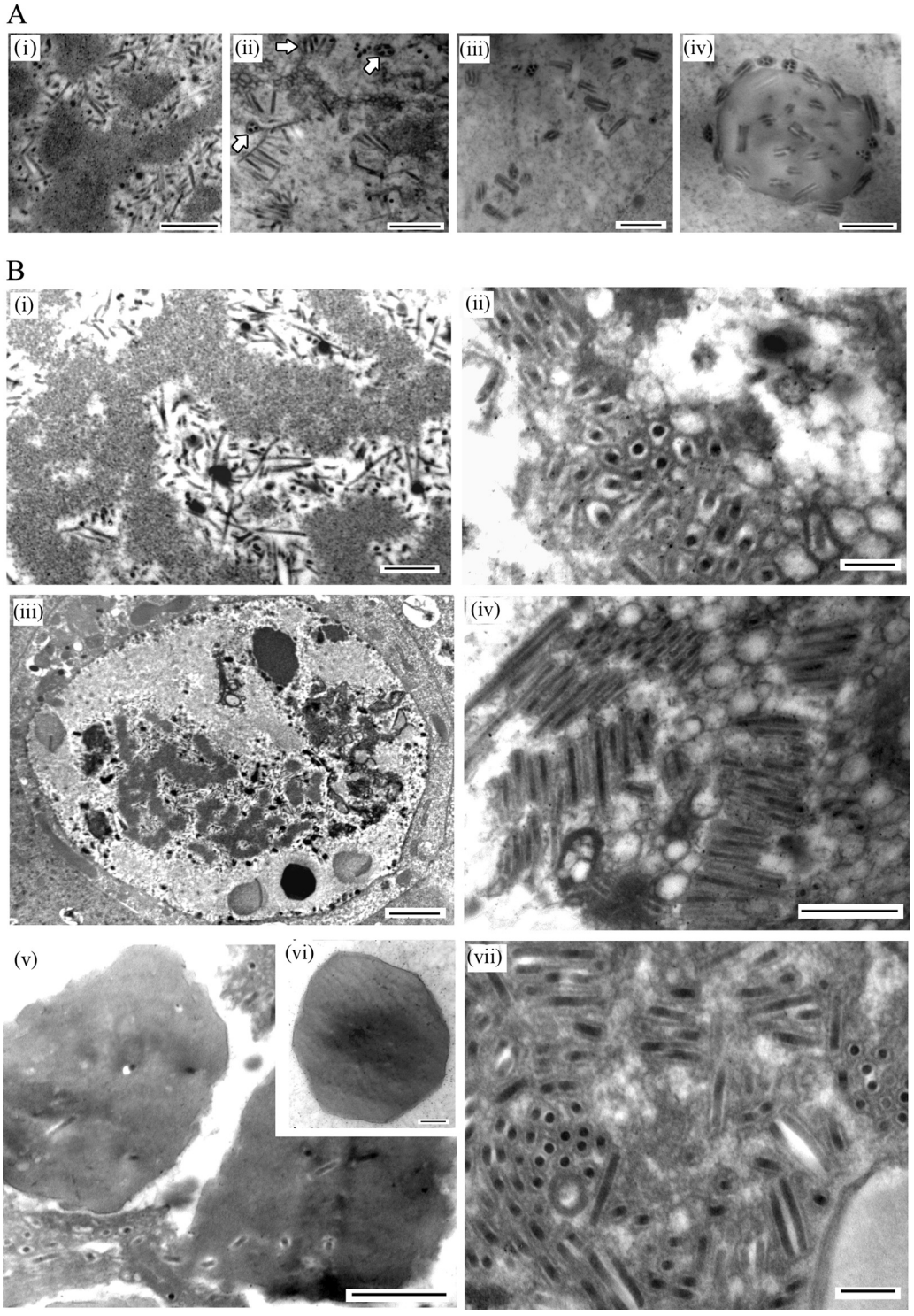

FIG. 7. Transmission electron microscopy analysis of cells transfected with AcWT-PG, Ac92KO-PG, or Ac92HAM1-PG DNA. (A) Cells transfected with AcWT-PG DNA and harvested at 72 h p.t. (i) Rod-shaped nucleocapsids in the virogenic stroma (VS). (ii) Intranuclear microvesicles and nucleocapsids aligning with the envelope in the ring zone. (iii) Matured multiply enveloped nucleocapsids of ODV in the ring zone. (iv) Polyhedrin with ODVs embedded. (B) (i to vi) Cells transfected with Ac92KO-PG. (i) Nucleocapsids in the VS. (ii and iv) Intranuclear microvesicles and singly enveloped nucleocapsids in the ODV in the ring zone. (iii) Cross section of a cell transfected with Ac92KO-PG DNA. (v and vi) Cross section of polyhedra with embedded singly enveloped nucleocapsids of the ODV (v) or without ODV (vi). (vii) Singly enveloped nucleocapsids in the ODV in the ring zone of Ac92HAM1-PG DNA-transfected cells. Bars represent 0.2 μm (B, panels ii, vi, and vii), 0.5 μm (A and B, panels i, iv, and v), or 2 μm (B, panel iii).

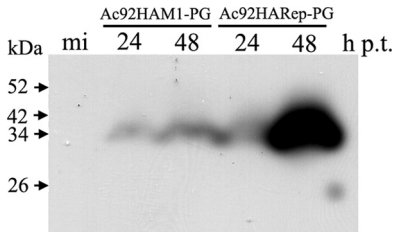

FIG. 8. Expression of Ac92 mutant in Ac92HAM1-PG-transfected cells. Cells were transfected with Ac92HAM1-PG or Ac92HARep-PG bacmid DNA and harvested at 24 and 48 h p.t. Total cellular proteins were immunoblotted using anti-HA antibody.

Cells were transfected with Ac92HARep-PG or Ac92HAM1-PG DNA and harvested at 24 and 48 h p.t., and proteins were detected by immunoblotting using anti-HA antibody. A specific immunoreactive band of approximately 33 kDa, corresponding to epitope-tagged Ac92, was detected in transfected cells (Fig. 8). The signal was stronger in Ac92HARep-PG DNA-transfected cells at 48 h p.t., probably due to virus spread to and protein production from adjacent cells, while there was no virus spread from Ac92HAM1-PG-transfected cells (data not shown and Fig. 3).

Replication of Ac92HAM1-PG in insect cells was similar to that of Ac92KO-PG (Fig. 3), including infection of single cells. In addition, plaques from Ac92HAM1-PG DNA-transfected cells consisted of single cells, reminiscent of those formed by Ac92KO-PG (Fig. 3B and C). Electron microscopy analysis of Ac92HAM1-PG DNA-transfected cells also showed results similar to those for Ac92KO-PG DNA-transfected cells, where singly enveloped nucleocapsids accumulated with microvesicles in the ring zone (Fig. 7B, panel vii). Thus, altering the C-X-X-C motif affected both BV production and ODV envelopment of multiple nucleocapsids, suggesting that sulfhydryl oxidase activity affected these processes.

Sulfhydryl oxidase activity of Ac92 ($C^{155}XXC^{158}$) and C-X-X-C ($A^{155}XXA^{158}$) mutant proteins. Ac92 (Ac92HA) and Ac92HA cysteine mutant protein (Ac92HAM1) were expressed in *E. coli* and affinity purified (data not shown). The purified proteins were assayed for sulfhydryl oxidase activity by using DTT as a substrate. Reactions were initiated by adding purified proteins to the substrate mixture, and aliquots were withdrawn at different times thereafter. The thiol content was measured in collected aliquots by DTNB reactivity (15). Ac92HA was able to oxidize DTT in a time-dependent manner and with similar oxidation efficiencies from 0 to 120 min, while Ac92HAM1 was not able to oxidize the substrate (Fig. 9). Thus, mutation of the C-X-X-C motif in Ac92 hinders sulfhydryl oxidase activity.

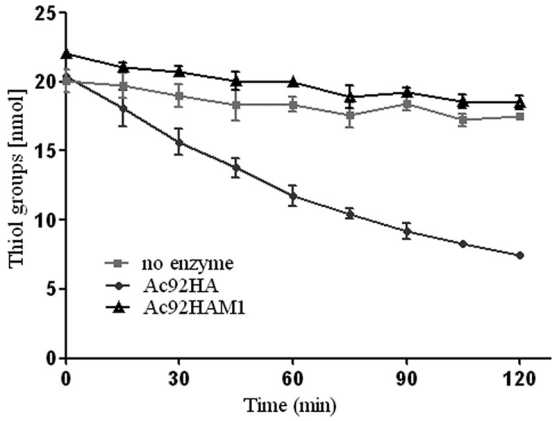

FIG. 9. Sulfhydryl oxidase activity of Ac92 (Ac92HA) and mutant (Ac92HAM1) proteins. Hexahistidyl-tagged proteins were expressed in *E. coli* and purified by nickel agarose. Sulfhydryl oxidase assays were carried out using 0.5 mM DTT as substrate, without recombinant protein (no enzyme), with epitope-tagged Ac92 (Ac92HA), or with Ac92 cysteine mutant protein (Ac92HAM1). Oxidation of thiol groups was measured spectroscopically at 412 nm after addition of 100 μM DTNB by determining the decrease of extinction at the indicated time points. The calculation of free thiol groups is described in Materials and Methods. The error bars represent standard deviations for two repeats.

DISCUSSION

The AcMNPV *ac92* is one of 31 baculovirus core genes, genes present in all sequenced baculovirus genomes (24). In this report, we investigated its enzymatic activity, transcription, and protein synthesis profiles and successfully generated recombinant viruses having an *ac92* gene missing or altered to study its function and effects on AcMNPV replication.

We mapped the *ac92* transcriptional start site to a late promoter element at nt 79622 (1). It is the furthermost of three such elements upstream of the gene. We confirmed that it is a late gene by its requirement for both DNA replication and protein synthesis. In addition, we found that Ac92 was not produced until 24 h p.i. Overall, these data are consistent with *ac92* belonging to the late gene phase.

Deletion of *ac92* led to a defect in infectious BV production. However, viral DNA replication was not affected, suggesting that a step after or not requiring viral DNA replication blocked BV production. The production of specific early and late gene protein products was also examined by immunoblotting. Production of neither IE-1 nor VP39 appeared to be affected by *ac92*.

Previous studies showed that Ac92 was associated with the ODV (3, 8, 18). Our results showed that Ac92 was a membrane component of BV and was associated with both the nucleocapsid and envelope of ODV. However, analysis of the sequence of Ac92 does not predict a transmembrane domain or signal sequence. Ac92 may be membrane associated.

During virus infection, an intranuclear viral replication center, the VS, is formed. Viral DNA replication and late gene transcription take place in the electron-dense VS (39). During the late phase of infection, viral DNA is condensed and packaged into capsids to form nucleocapsids within the VS. These nucleocapsids egress from the cell nucleus to bud through a modified plasma membrane to form BV. Later in infection, nucleocapsids remain in the nucleus and become bundled together, and it is thought that they acquire envelopes from intranuclear microvesicles to form ODVs. The resulting ODVs are embedded within large proteinaceous paracrystalline occlusion bodies (36). Our data showed that the deletion of *ac92* did not affect the formation of VS, nucleocapsid assembly, the formation of intranuclear microvesicles, or polyhedra (Fig. 7). Interestingly, when cells were transfected with DNA from Ac92KO-PG, multiply enveloped nucleocapsids of the ODV

were not observed; instead, we observed what appeared to be singly enveloped nucleocapsids in the ring zone associated with intranuclear microvesicles. Consistent with this result, Ac92 localizes to the ring zone of infected cells (D. A. Theilmann, personal communication). It would be interesting to know if these singly enveloped nucleocapsids are orally infectious to insect larvae and how their infectivity compares to that of multiply enveloped nucleocapsids.

Alignments between Ac92 homologs predicted in the genomes of all sequenced M and S phenotype baculoviruses did not show any significant differences that could provide insight into a relationship between the gene and the phenotype (results not shown). Although lack of *ac92* affects virion assembly resembling S-like phenotype virions, since *ac92* is carried in both S and M phenotype baculoviruses, we do not think that it is a direct determinant of the M virion phenotype. There is no information available concerning factors affecting the M virus phenotype.

A previous study determined that Ac92 had a 90% probability of being an FAD-binding sulfhydryl oxidase related to the ERV/ALR family (24). This relationship was based on the prediction of helical domains surrounding a C-X-X-C motif with potential oxidoredox activity (15). Ac92 was expressed and purified, and its biophysical and enzymatic properties were characterized to confirm that it indeed encoded an FAD-containing sulfhydryl oxidase (15). In the present study, mutation of the C-X-X-C sulfhydryl oxidase motif in *ac92* abolished the ability of Ac92 to oxidize DTT, confirming that the cysteine motif is important for sulfhydryl oxidase activity in Ac92 and is essential for function. Our data showed that Ac92HAM1-PG had characteristics similar to those of the knockout virus. Although we cannot rule out that this mutation resulted in a misfolded protein, it suggests that the sulfhydryl oxidase activity might play a major role in virus formation and infectivity.

In vaccinia virus, three proteins, E10R, A2.5L, and G4L, comprise a complete pathway for the formation of disulfide bonds in intracellular virion membrane proteins (26–28, 35). The upstream component, E10R, belongs to the ERV1/ALR family of FAD-containing sulfhydryl oxidases, participates in disulfide bond formation, is associated with virion membranes, and has a role in virion morphogenesis (26, 27). The second component, A2.5L, is a small α-helical protein with a C-X-X-X-C motif that forms a stable disulfide-linked heterodimer with E10R and a transient disulfide-linked complex with the third component, G4L (28). G4L is a thioredoxin-like protein that directly oxidizes thiols of L1R, the virion membrane protein (28); F9L, a virion structurally related protein (28); and A28L, another virion membrane-associated protein (25). These proteins involved in a disulfide bond formation pathway are conserved throughout the poxvirus family, suggesting that the pathway is an ancestral mechanism in this group of viruses (28). In African swine fever virus, the protein pB119L, with a C-X-X-C motif similar to that of E10R and belonging to the ERV/ALR family of sulfhydryl oxidases, has been described as a late nonstructural protein required for virion maturation (12). Biochemical experiments showed that pB119L is an FAD-containing sulfhydryl oxidase that interacts with a viral protein, A151R. A151R was found to interact with the viral structural protein pE248R, which contains disulfide bridges and belongs to a class of myristoylated proteins related to vaccinia virus L1R (21, 22). Vaccinia virus replicates in the cytoplasm of infected cells in contrast to baculovirus nuclear replication. It is interesting that both viruses require sulfhydryl oxidase activity for virus morphogenesis in distinct nonoptimal redox cellular compartments.

Ac92 has redox functions necessary for virus morphogenesis. Ac92 shares functional properties and has localization similar to those of other viral sulfhydryl oxidases. Substrates of Ac92 will help to elucidate the mechanisms and requirements for virion assembly in baculoviruses.

ACKNOWLEDGMENTS

We thank Kai Yang (Sun Yat-sen University) for his generous gifts of pFB1-PH-GFP plasmid and the VP39 polyclonal antiserum and Linda Guarino (Texas A&M) for IE-1 antibodies. We also thank George R. Rohrmann (Oregon State University) for discussions and David A. Theilmann for communicating results prior to publication.

This research was supported by the United States Department of Agriculture 2008-35302-18849 award.

This is contribution number 10-388-J from the Kansas Agricultural Experiment Station.

REFERENCES

1. **Ayres, M. D., S. C. Howard, J. Kuzio, M. Lopez-Ferber, and R. D. Possee.** 1994. The complete DNA sequence of *Autographa californica* nuclear polyhedrosis virus. Virology **202:**586–605.
2. **Bideshi, D. K., and B. A. Federici.** 2000. The *Trichoplusia ni* granulovirus helicase is unable to support replication of *Autographa californica* multicapsid nucleopolyhedrovirus in cells and larvae of *T. ni*. J. Gen. Virol. **81:**1593–1599.
3. **Braunagel, S. C., W. K. Russell, G. Rosas-Acosta, D. H. Russell, and M. D. Summers.** 2003. Determination of the protein composition of the occlusion-derived virus of *Autographa californica* nucleopolyhedrovirus. Proc. Natl. Acad. Sci. U. S. A. **100:**9797–9802.
4. **Braunagel, S. C., and M. D. Summers.** 1994. *Autographa californica* nuclear polyhedrosis virus, PDV, and ECV viral envelopes and nucleocapsids: structural proteins, antigens, lipid and fatty acid profiles. Virology **202:**315–328.
5. **Carstens, E. B., and Y. Wu.** 2007. No single homologous repeat region is essential for DNA replication of the baculovirus *Autographa californica* multiple nucleopolyhedrovirus. J. Gen. Virol. **88:**114–122.
6. **Chiu, J., D. Tillett, I. W. Dawes, and P. E. March.** 2008. Site-directed, ligase-independent mutagenesis (SLIM) for highly efficient mutagenesis of plasmids greater than 8kb. J. Microbiol. Methods **73:**195–198.
7. **Crouch, E. A., and A. L. Passarelli.** 2002. Genetic requirements for homologous recombination in *Autographa californica* nucleopolyhedrovirus. J. Virol. **76:**9323–9334.
8. **Deng, F., R. Wang, M. Fang, Y. Jiang, X. Xu, H. Wang, X. Chen, B. M. Arif, L. Guo, H. Wang, and Z. Hu.** 2007. Proteomics analysis of *Helicoverpa armigera* single nucleocapsid nucleopolyhedrovirus identified two new occlusion-derived virus-associated proteins, HA44 and HA100. J. Virol. **81:**9377–9385.
9. **Detvisitsakun, C., M. F. Berretta, C. Lehiy, and A. L. Passarelli.** 2005. Stimulation of cell motility by a viral fibroblast growth factor homolog: proposal for a role in viral pathogenesis. Virology **336:**308–317.
10. **Herniou, E. A., J. A. Olszewski, J. S. Cory, and D. R. O'Reilly.** 2003. The genome sequence and evolution of baculoviruses. Annu. Rev. Entomol. **48:**211–234.
11. **Jehle, J. A., G. W. Blissard, B. C. Bonning, J. S. Cory, E. A. Herniou, G. F. Rohrmann, D. A. Theilmann, S. M. Thiem, and J. M. Vlak.** 2006. On the classification and nomenclature of baculoviruses: a proposal for revision. Arch. Virol. **151:**1257–1266.
12. **Lewis, T., L. Zsak, T. G. Burrage, Z. Lu, G. F. Kutish, J. G. Neilan, and D. L. Rock.** 2000. An African swine fever virus ERV1-ALR homologue, 9GL, affects virion maturation and viral growth in macrophages and viral virulence in swine. J. Virol. **74:**1275–1285.
13. **Li, L., Z. Li, W. Chen, and Y. Pang.** 2007. Cloning, expression of *Autographa californica* nucleopolyhedro virus *vp39* gene in *Escherichia coli* and preparation of its antibody. Biotechnology (NY) **17:**5–7.
14. **Li, Y., J. Wang, R. Deng, Q. Zhang, K. Yang, and X. Wang.** 2005. vlf-1 deletion brought AcMNPV to defect in nucleocapsid formation. Virus Genes **31:**275–284.
15. **Long, C. M., G. F. Rohrmann, and G. F. Merrill.** 2009. The conserved baculovirus protein p33 (Ac92) is a flavin adenine dinucleotide-linked sulfhydryl oxidase. Virology **388:**231–235.

16. **Monsma, S. A., A. G. Oomens, and G. W. Blissard.** 1996. The GP64 envelope fusion protein is an essential baculovirus protein required for cell-to-cell transmission of infection. J. Virol. **70:**4607–4616.
17. **O'Reilly, D. R., L. K. Miller, and V. A. Luckow.** 1992. Baculovirus expression vector: a laboratory manual. W. H. Freeman and Co., New York, NY.
18. **Perera, O., T. B. Green, S. M. Stevens, Jr., S. White, and J. J. Becnel.** 2007. Proteins associated with *Culex nigripalpus* nucleopolyhedrovirus occluded virions. J. Virol. **81:**4585–4590.
19. **Potter, K. N., and L. K. Miller.** 1980. Transfection of two invertebrate cell lines with DNA of *Autographa californica* nuclear polyhedrosis virus. J. Invertebr. Pathol. **36:**431–432.
20. **Prikhod'ko, G. G., Y. Wang, E. Freulich, C. Prives, and L. K. Miller.** 1999. Baculovirus p33 binds human p53 and enhances p53-mediated apoptosis. J. Virol. **73:**1227–1234.
21. **Rodriguez, I., M. L. Nogal, M. Redrejo-Rodriguez, M. J. Bustos, and M. L. Salas.** 2009. The African swine fever virus virion membrane protein pE248R is required for virus infectivity and an early postentry event. J. Virol. **83:** 12290–12300.
22. **Rodriguez, I., M. Redrejo-Rodriguez, J. M. Rodriguez, A. Alejo, J. Salas, and M. L. Salas.** 2006. African swine fever virus pB119L protein is a flavin adenine dinucleotide-linked sulfhydryl oxidase. J. Virol. **80:**3157–3166.
23. **Rohrmann, G. F.** 1986. Evolution of occluded baculoviruses, p. 203–315. *In* R. R. Granados and B. A. Federici (ed.), The biology of baculoviruses, vol. 1. CRC Press, Inc., Boca Raton, FL.
24. **Rohrmann, G. F.** 2008. Baculovirus molecular biology. National Library of Medicine (US), National Center for Biotechnology Information, Bethesda, MD.
25. **Senkevich, T. G., B. M. Ward, and B. Moss.** 2004. Vaccinia virus A28L gene encodes an essential protein component of the virion membrane with intramolecular disulfide bonds formed by the viral cytoplasmic redox pathway. J. Virol. **78:**2348–2356.
26. **Senkevich, T. G., A. S. Weisberg, and B. Moss.** 2000. Vaccinia virus E10R protein is associated with the membranes of intracellular mature virions and has a role in morphogenesis. Virology **278:**244–252.
27. **Senkevich, T. G., C. L. White, E. V. Koonin, and B. Moss.** 2000. A viral member of the ERV1/ALR protein family participates in a cytoplasmic pathway of disulfide bond formation. Proc. Natl. Acad. Sci. U. S. A. **97:** 12068–12073.
28. **Senkevich, T. G., C. L. White, E. V. Koonin, and B. Moss.** 2002. Complete pathway for protein disulfide bond formation encoded by poxviruses. Proc. Natl. Acad. Sci. U. S. A. **99:**6667–6672.
29. **Sevier, C. S., and C. A. Kaiser.** 2002. Formation and transfer of disulphide bonds in living cells. Nat. Rev. Mol. Cell Biol. **3:**836–847.
30. **Vanarsdall, A. L., K. Okano, and G. F. Rohrmann.** 2005. Characterization of the replication of a baculovirus mutant lacking the DNA polymerase gene. Virology **331:**175–180.
31. **Vaughn, J. L., R. H. Goodwin, G. J. Tompkins, and P. McCawley.** 1977. The establishment of two cell lines from the insect *Spodoptera frugiperda* (Lepidoptera; Noctuidae). In Vitro **13:**213–217.
32. **Washburn, J. O., E. H. Lyons, E. J. Haas-Stapleton, and L. E. Volkman.** 1999. Multiple nucleocapsid packaging of *Autographa californica* nucleopolyhedrovirus accelerates the onset of systemic infection in *Trichoplusia ni*. J. Virol. **73:**411–416.
33. **Washburn, J. O., D. Trudeau, J. F. Wong, and L. E. Volkman.** 2003. Early pathogenesis of *Autographa californica* multiple nucleopolyhedrovirus and *Helicoverpa zea* single nucleopolyhedrovirus in *Heliothis virescens*: a comparison of the 'M' and 'S' strategies for establishing fatal infection. J. Gen. Virol. **84:**343–351.
34. **Whitby, P. W., D. J. Morton, and T. L. Stull.** 1998. Construction of antibiotic resistance cassettes with multiple paired restriction sites for insertional mutagenesis of *Haemophilus influenzae*. FEMS Microbiol. Lett. **158:**57–60.
35. **White, C. L., T. G. Senkevich, and B. Moss.** 2002. Vaccinia virus G4L glutaredoxin is an essential intermediate of a cytoplasmic disulfide bond pathway required for virion assembly. J. Virol. **76:**467–472.
36. **Williams, G. V., and P. Faulkner.** 1997. Cytological changes and viral morphogenesis during baculovirus infection, p. 61–107. *In*: L. K. Miller (ed.), The baculoviruses. Plenum Press, New York, NY.
37. **Wu, W., H. Liang, J. Kan, C. Liu, M. Yuan, C. Liang, K. Yang, and Y. Pang.** 2008. *Autographa californica* multiple nucleopolyhedrovirus 38K is a novel nucleocapsid protein that interacts with VP1054, VP39, VP80, and itself. J. Virol. **82:**12356–12364.
38. **Wu, W., T. Lin, L. Pan, M. Yu, Z. Li, Y. Pang, and K. Yang.** 2006. *Autographa californica* multiple nucleopolyhedrovirus nucleocapsid assembly is interrupted upon deletion of the 38K gene. J. Virol. **80:**11475–11485.
39. **Young, J. C., E. A. Mackinnon, and P. Faulkner.** 1993. The architecture of the virogenic stroma in isolated nuclei of *Spodoptera frugiperda* cells *in vitro* infected by *Autographa californica* nuclear polyhedrosis virus. J. Struct. Biol. **110:**141–153.